Journal of Polymers and the Environment (2022) 30:4377–4393
https://doi.org/10.1007/s10924-022-02514-1

ORIGINAL PAPER

An Experimental and Metamodeling Approach to Tensile Properties of Natural Fibers Composites

Mohamad Alhijazi[1] · Babak Safaei[1,2] · Qasim Zeeshan[1] · Mohammed Asmael[1] · Mohammad Harb[3] · Zhaoye Qin[4]

Accepted: 14 June 2022 / Published online: 11 July 2022

Abstract

The present work presents an analysis of the tensile properties of Palm as well as Luffa natural fiber composites (NFC) in high density polyethylene (HDPE), polypropylene (PP), Epoxy, and Ecopoxy (BioPoxy 36) matrixes, taking into consideration the effect of fibers volume fraction variation. Finite element analysis i.e. representative volume element (RVE) model with chopped random fiber orientation was utilized for predicting the elastic properties. Tensile test following ASTM D3039 standard was conducted. Artificial neural network, multiple linear regression, adaptive neuro-fuzzy inference system, and support vector machine were implemented for defining the design space upon the considered parameters and evaluating the reliability of these machine learning approaches in predicting the tensile strength of natural fibers composites. Furthermore, BioPoxy 36 with 0.3 luffa fibers exhibited the highest tensile strength. Finite element analysis (FEA) findings profusely agreed with the experimental results. ANFIS Machine Learning (ML) tool showed least prediction error in predicting tensile strength of natural fibers composites.

Keywords Palm fibers · Luffa fibers · Tensile properties · Finite element analysis · Machine learning

Introduction

Natural fibers' composite material attained a notable attention in materials' science area due to their profuse advantages i.e. light weight, low density, high strength to weight ratio, environmental-friendly, low cost, and their availability in the nature. Moreover, natural fibers like sisal, coir, kenaf, palm, bamboo, jute, hemp, and luffa were vastly considered in engineering and science researches. In consequence of the environmental awareness throughout the last two decades, development of a recyclable and environmental-friendly composite material has drastically increased [1]. Discovering a new alternative material to the widely utilized materials like metals, synthetic fiber composites, and alloys has become the prevalent research area in academia as well as in the industry [2, 3]. Furthermore, studies on the application of natural fibers i.e. wood, pineapple, luffa, feather, palm, jute, animal silk, and so on became widespread among scientists and engineers, due to their merits, such as; low electricity usage for producing these natural fibers [4], less tool wear comparing with that involved in processing synthetic fibers' composites [5–7], less harmful gases emission when burned at end of life or exposed to high-heat [8], lower hazards throughout the production process, cheaper than synthetic fibers [9], notable strength, low density, and high stiffness [10]. Recently, natural fibers composites made of kenaf, jute, sisal, hemp, flax [10, 11] have been increasingly involved in various engineering fields i.e. circuit boards, building materials, automotive, etc. [12–14]. Short service life, high water and moisture absorption, micro-organisms and sunrays degradation are main constraints of expanding the production of natural fiber composites (NFCs) [15], yet a suitable development of NFCs is able to let these green composite to emerge into new markets and attain bigger demand [16–19].

✉ Babak Safaei
babak.safaei@emu.edu.tr

1 Department of Mechanical Engineering, Eastern Mediterranean University, North Cyprus via Mersin 10, Famagusta, Turkey

2 Department of Mechanical Engineering Science, University of Johannesburg, Gauteng 2006, South Africa

3 Department of Mechanical Engineering, American University of Beirut, Beirut, Lebanon

4 State Key Laboratory of Tribology, Department of Mechanical Engineering, Tsinghua University, Beijing, China

World widely, date palm trees produce more than 8 million tons of date fruits every year, thereby keeping tones of fibrous wastes. A natural woven mat surrounds the trunk of date palm, the aforementioned is generally involved in ropes and baskets production. Cucurbitaceae family includes a subcategory called luffa, its unripe fruit is used in Chinese, Indian, and Vietnamese dishes. While its mature fruit is widely used as a shower sponge and further household utilizations. The three-dimensional network structure of luffa leads to its high strength, toughness and stiffness [20, 21]. Taban et al. [19] proposed replacing synthetic fibers by palm fibers in acoustic isolation applications. Shalwan et al. [22] mentioned an increase in the tensile strength of epoxy from 58 to 68 MPa by adding date palm fibers. Ibrahim et al. [23] observed that increasing the date palm fibers' volume fraction up to 0.5 increases the tensile strength and young's modulus. Shen et al. [24] highlighted the notable behavior of luffa natural fibers composites in acoustic and vibrations applications. While Mani et al. [25] observed an increase in the tensile strength of luffa NFC by increasing fibers' content up to 40% in epoxy matrix. The significant growth in NFCs utilization evidences the requirement of an efficient design and development of the composites in order to achieve optimal characteristics. Researchers in natural fibers composites area applied computational techniques i.e. numerical and analytical, in order to simulate thermal, physical, and mechanical properties while developing a new NFC [26–28]. Moreover, studies mainly focused on predicting the micromechanical properties of NFCs, yet, simulation findings exhibited significant prediction accuracy and profusely agreed with the experimental results. For instance, Parsad et al. [29] concluded that the finite element analysis results of luffa NFC agreed with the experimental findings. Similarly, Sowmya et al. [30] spotted the light on the strong capability of Finite element analysis in predicting the mechanical characteristics of hemp natural fibers' composite, thus, finite element analysis (FEA) findings displayed significant agreement with experimental results. However, representative volume element estimates the characteristics of a composite material unit cells at macro-, nano-, and micro-scale. Representative volume element is the major effective homogenized multiscale FEA, therefore it has to be firstly applied for the analysis of composite materials with complex structures like NFC which contain diverse length scales [31–36].

Previously machine learning was utilized for detecting C60 solubility, however it is currently involved in predicting molecular characteristics of designed materials. Despite the fact that experimental testing is significantly essential for developing a new material, machine learning contributes in decreasing the cost as well as the computational time throughout an experiment, as the required tools for running the machine learning algorithms are free to access and easily available [12, 37–40]. Recently, artificial intelligence was applied by several researchers in composite materials and natural fibers composites. Antil et al. [41] utilized artificial neural network (ANN) and RSM to study the erosion behavior of S Glass composites, inputs included nozzle diameter, impingement angle, and slurry pressure. Pati et al. [42] applied ANN for predicting the wear behavior of glass/epoxy composites, input parameters consisted of; erodent temperature, erodent size, RBD content, impingement angle, and impact velocity. While Baseer et al. [43] assigned shear strength, failure stress and strain, tensile modulus, and tensile strength as input parameters for evaluating the interfacial and tensile properties of hybrid composite material. Atuanya et al. [44] emphasized the reliability of using ANN to predict the mechanical behavior of NFCs, authors implemented artificial neural networks for predicting the mechanical properties of date fibers' reinforced low-density polyethylene (recycled), input data consisted of fibers' weight percentages, while the output was tensile strength, young's modulus, elongation, flexural modulus, and hardness. Daghigh et al. [45] utilized K-Nearest Neighbor Regressor for predicting the heat deflection temperature of latania NFCs, pistachio shell NFCs, and date seed NFCs. Also, Daghigh et al. [46] applied decision tree regressor and adaptive boosting regressor for studying the fracture toughness of the aforementioned natural fibers composites. Garg et al. [47] implemented extreme machine learning to investigate the mechanical factor of Jute as well as Coir natural fibers composites. Wang et al. [48] used random forest machine learning approach for analyzing the acoustic emission of Flax NFCs.

The aim of this study was to investigate the elastic properties of palm and luffa NFCs in BioPoxy 36, Epoxy, Polypropylene, and High-Density Polyethylene matrixes by modeling and simulating the micro-mechanical properties of NFC using FEA representative volume element (RVE) chopped fibers' orientation, validating the optimal configuration by experimentally testing it and validating its mechanical properties (Tensile ASTM D3039), and developing an Artificial Neural Networks, Multiple Linear Regression, Adaptive Neuro-Fuzzy Inference System, and Support Vector Machine based Metamodel. Impact of increasing fiber content was identified through assigning multiple fibers volume fractions i.e. 0.1, 0.2, 0.3.

Experimental Procedure

In this research, date palm meshes and luffa were considered as reinforcements, while BioPoxy 36, epoxy, polypropylene, high density polyethylene were selected as a matrix. This section describes main stages of tensile testing samples' preparation, which include; fibers' extraction, matrixes materials' supply, molds' preparation, and natural fibers composite specimens' preparation. Figure 1 describes the main stages of tensile testing procedure.

Materials and Fibers' Preparation

Date palm meshes that surround the stem were extracted from a palm tree located in north Lebanon, the fibers were kept to dry for 72 h and then washed with cold water in order to remove all the dust and impurities. Next, the cleaned palm fibers were dried through placing them under the sunlight on a mosquito net for 23 days [49]. The aim of using a mosquito net was to let the air ventilate the bottom of palm fibers, and avoid any water drop from staying below the fibers, which thereby could harm the fibers by creating moisture. Luffa sponge was supplied from a local store, it was dry and peeled, its length was 46 cm and its average diameter was 16 cm. Regarding the matrixes, BioPoxy 36 was offered by the manufacturer of this green resin i.e. EcoPoxy, Canada. Aquaglass epoxy resin and its hardener were supplied from Colortek, Lebanon. Moreover, polypropylene 528 k and high-density polyethylene F00952 were supplied from Sabic.

Molds Development

Since both thermoplastic and thermoset matrixes are considered in this research, and each of the aforementioned has its specific preparation technique, therefore it was compulsory to utilize two different mold's types. For natural fibers' reinforced thermosets, 36 silicon molds were developed by the following steps: (1) silicon sealant was added into water/dish soap mixture, (2) putty was then mixed well till it reached an unsticky dough structure, (3) next, a wooden pattern that has same dimensions of the specimens was inserted in the putty and pressed well around the corners, (4) lastly, the putty

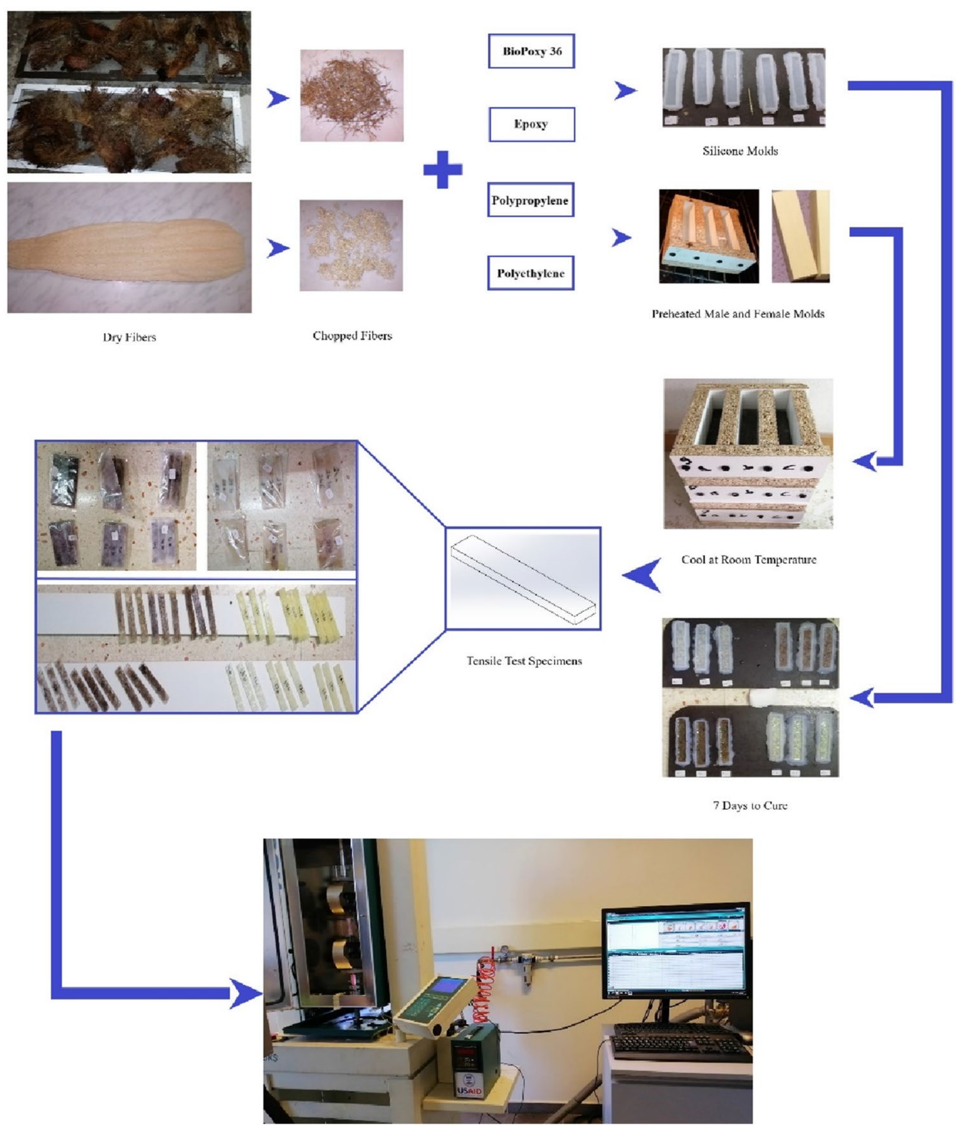

Fig. 1 Palm and luffa NFCs specimens' preparation and testing

was rested on a plastic tray for 15 min to dry before removing the pattern. Meanwhile for the thermoplastic NFCs, the mold required a female mold along with its male part that contributes in compressing the molten NFC till it solidifies. Hence, a plywood board was trimmed into small parts that included the inner and outer walls of the mold, and their base. Thereby, these parts were assembled using wood screws to create 15 female molds that consist of 3 cavities each.

Samples Preparation

Luffa as well as date palm fibers were chopped using a waring blender in order to have a homogeneous mixture with the considered matrixes, the approximate fibers' dimensions were 1 cm length and 0.5 mm diameter, and the desired fibers' orientation was random (Fig. 1). In terms of NFCs with thermoset matrixes, the resin was mixed with its hardener for 5 min, the resin to hardener mixing ratio was 4:1 for BioPoxy 36 and 1.8:1 for epoxy. 0.1, 0.2, 0.3 fibers' volume fractions were considered in for the experimental specimens. Since the molds may have a small variety in their heights, the specimens' thickness was ensured using a tiny stick marked on 5 mm from its tip. First, coat of silicone spray was applied to the bottom of the mold and a small layer of resin/hardener mixture was poured, then the fibers were added upon a specific volume fraction i.e. 0.1, 0.2, or 0.3, next, the remaining quantity of the resin was added and the fibers were pushed downward in order to release any available air bubbles. The specimens were prepared at a room temperature of 21 ℃ and humidity of 66%, all 36 specimens were kept for 1 week to fully cure. Regarding the specimens with PP matrix, the granules were put in an aluminum foil sprayed with silicone realizing agent, and then placed in a toaster at 230 ℃ for 5 min to melt, then the fibers were added into the molten plastic and kept in the toaster for 3 more minutes for getting the most soft structure that helps in taking the mold's shape, next, the molten NFC was placed in a preheated female mold at 80 ℃ and pressed using a screw clamp on the male part of the mold. Thus, the aforementioned NFC was cooled down inside the mold for 15 min at a room temperature of 18 ℃. Meanwhile, specimens with HDPE matrix were prepared through similar process, yet the first melting stage took 3 min, and 2 min after adding the fibers, which was due to the low melting temperature of HDPE (190 ℃). Furthermore, specimens' dimensions were $120 \times 20 \times 5$ mm following the ASTM 3039 standard. A total of 72 samples were prepared for the tensile test by considering 8 different NFCs i.e. palm/epoxy, palm/BioPoxy, palm/PP, palm/HDPE, luffa/epoxy, luffa/BioPoxy, luffa/PP, and luffa/HDPE with fibers volume fraction of 0.1, 0.2, and 0.3. Thus, each NFC combination had 3 replicated samples.

Tensile Test

The tensile test was conducted using a Hounsfield universal machine and a laser extensometer. Two reflective tapes were taped to each specimen in order to test strain variations through the extensometer. The considered gage length was 60 mm, and the speed rate was 5 mm/min [50]. Following ASTM D3039 standard regarding chopped and randomly oriented composite materials, both sides of all 72 specimens were covered with emery cloth (grade 100 sand papers), which contributed in increasing the grip and preventing the samples from slipping out of the machine clamps. After tightening the machine clamps on the specimens' edges, the applied force as well as the strain rate were adjusted to be zero. Hence, tension load was applied upon the specified speed rate and the specimens extended till failure. Results were revealed through stress–strain graphs as well as excel files that included whole details of force, break distance, ultimate tensile strength, and strain.

Finite Element Analysis

Selected materials in this research in the numerical analysis are: BioPoxy 36, epoxy, high density polyethylene and polypropylene as a matrix and date palm and luffa fibers as a reinforcement. The matrixes and fibers were assumed to be homogenized and isotropic. Different fiber volume fractions were considered (0.1 to 0.3) in order to evaluate the effect of fiber content on NFC elastic properties. RVE with random chopped orientations was implemented for predicting the elastic properties of BioPoxy/palm, BioPoxy/luffa, Epoxy/palm, Epoxy/luffa, PP/palm, PP/luffa, HDPE/palm, and HDPE/luffa. Figure 2 shows the utilized representative volume element unit cell.

ANSYS "Materials Designer" tool was utilized, which automatically applies the approach of representative volume element homogenization method. Fibers' diameter was considered to be 5 µm and the RVE geometry was assigned to be square. Fibers' to matrix bonding was considered to be free of flaws, and the natural fibers composites were considered to be free of voids. Meshing type utilized for the representative volume element was conformal. Furthermore, Orthotropic output of RVE chopped was assigned into a $120 \times 20 \times 5$ mm beam (following ASTM D3039), thereby a tensile load was applied on the beam till its failure in order to measure its tensile strength. Materials properties considered for the simulation are displayed in Table 1.

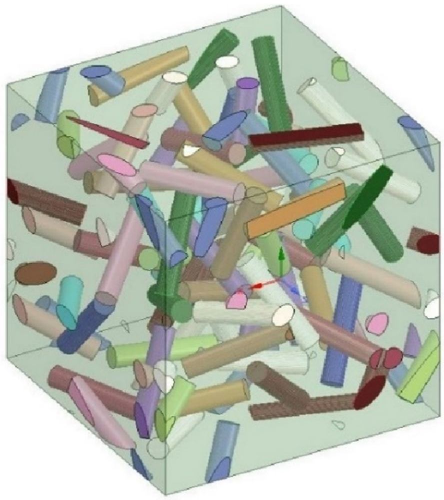

Fig. 2 RVE with randomly oriented chopped fibers

Table 1 Input properties of the selected materials for simulation

Materials	Young's modulus	Poisson's ratio
Date Palm	700 MPa	0.19
Luffa	80 MPa	0.3
BioPoxy 36	1850 MPa	0.3
Epoxy	23 MPa	0.3
PP	630 MPa	0.3
HDPE	150 MPa	0.28

Machine Learning Models

Machine learning is a subcategory of artificial intelligence, it is a technique where the computers learn the way of doing something that is generally particular to human and gained through experience. Usually, the efficiency of the algorithm increases by increasing the quantity of learning samples [51]. Deep learning became popular in many research areas since 2006, where it was implemented for determining the performance in fields like speech recognition, object recognition, image segmentation, and machine translation. Majority of deep learning approaches are usually presented as deep neural networks as they involve neural network architecture. There are two types of machine learning algorithms, supervised and unsupervised. Supervised machine learning proved its convenience in most manufacturing applications as the aforementioned provide labeled data [52].

$$\text{Prediction error } \% = \frac{|Expt.Value - Pred.Value|}{Expt.Value} \times 100 \tag{1}$$

Prediction error is a simple method that evaluates the reliability of a training model, where the prediction model is validated through new input data that were unconsidered previously in testing the model. Therefore, the error percentage of a training model can be defined using this tool. Moreover, a common technique for defining the error of a model is Root Mean Square Error (RMSE).

$$\text{RMSE} = \sqrt{\frac{1}{N}\sum_{i-1}^{N}(pi - qi)^2} \tag{2}$$

where qi is the actual value, pi is the prediction of the deliberate information, and N is the complete training data.

Artificial neural network, Response Surface metamodel, adaptive neuro-fuzzy inference system, and support vector machine were implemented in this research to define the design space upon the considered parameters, and determine most convenient approach in predicting tensile strength values of input parameters that were unconsidered in the experimental tensile test of natural fibers composites. Inputs of the proposed model are matrix types, fibers' types, and fibers' volume fraction. Results of all experimentally tested specimens were applied for training, testing, and validation. Reliability of TS prediction model was evaluated using the mean absolute percentage error.

Results and Discussion

This section presents results of tensile properties obtained from tensile test experiment, finite element analysis, and machine learning of palm and luffa NFCs in Epoxy, BioPoxy 36, HDPE and PP matrices.

Tensile Test Results

Tensile test findings are listed in this section, which includes tensile strength, strain, and young's modulus of luffa as well as palm natural fibers composites in BioPoxy, epoxy, HDPE and PP matrices. First, some stress and strain charts are displayed to show the tensile behavior of these NFCs, then the effect of increasing the natural fibers volume fraction in the considered matrices. Figure 3 shows the stress–strain behavior of BioPoxy NFC with 0.1 luffa fibers.

As shown in Fig. 3, the stress increased gradually to reach a yield strength of 3.77 MPa at 0.262%, then it followed a continuous increase to attain an ultimate tensile strength of 35.3 MPa at 4.31% straight before its brittle failure. The stress and strain behavior of palm/biopoxy NFC at 0.3 is shown in Fig. 4.

As shown in Fig. 4, ecopoxy with 0.3 palm NFC recorded a yield strength of 2.89 MPa at 0.135%, thereby the stress increased notably to reach an ultimate tensile strength of 20.2 MPa at 2.51%, thus, a brittle failure was observed at a

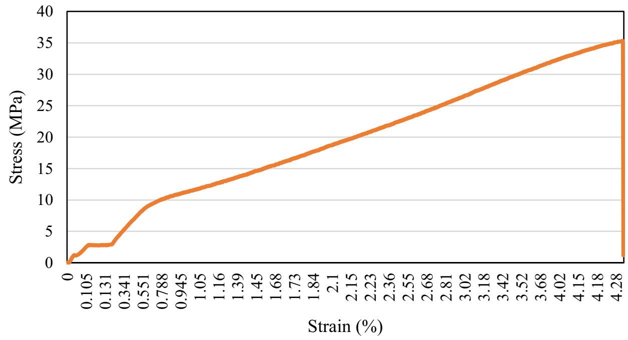

Fig. 3 Stress and strain curve of luffa/biopoxy "0.1"

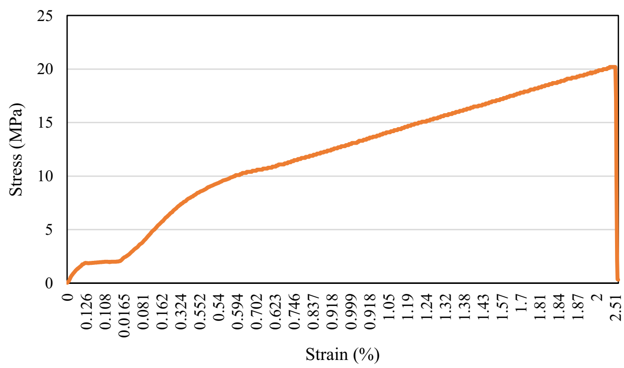

Fig. 4 Stress and strain curve of palm/biopoxy "0.3"

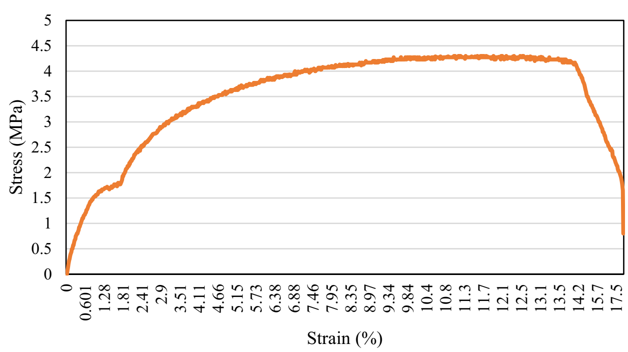

Fig. 5 Stress and strain curve of palm/epoxy "0.3"

strain of 2.78%. Figure 5 displays the stress–strain behavior of epoxy NFC with 0.3 palm.

As exhibited in Fig. 5, a yield strength of 1.67 MPa was observed at 1.8%, then the stress increased to reach a 4.13 MPa ultimate tensile strength at 14.1%, which emphasizes the notable ductility of this material, thereby the Palm/Epoxy NFC performed a plastic failure at 17.5%. Figure 6 shows the stress and strain behavior of epoxy natural fibers composite with 0.3 luffa fibers.

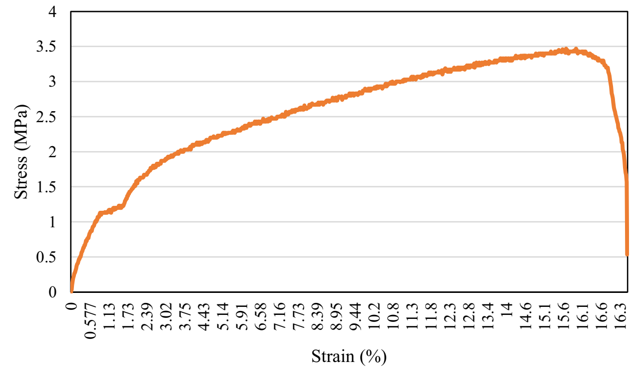

Fig. 6 Stress and strain curve of luffa/epoxy "0.3"

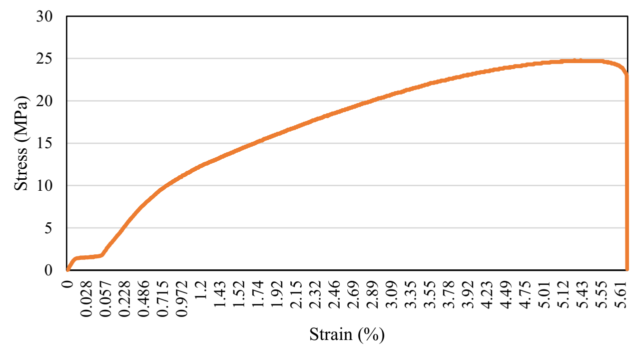

Fig. 7 Stress and strain curve of palm/PP "0.1"

As Fig. 6 shows, the stress increased gradually and a yield strength of 1.5 MPa was exhibited at 1.22%, then the stress continued increasing along with a notable increment in the strain, hence an ultimate tensile strength of 3.43 MPa was observed at 16.1%. Figure 7 displays the stress–strain curve of polypropylene NFC with 0.1 palm fibers.

As exhibited in Fig. 7, polypropylene with 0.1 pam fibers revealed a yield strength of 3.07 at 0.143%, then the stress drastically increased to attain an ultimate tensile strength of 24.7 MPa at 5.52%, next it decreased to 23 MPa at 5.58% right before its brittle failure at 5.61%. The stress and strain behavior of luffa/PP NFC at 0.1 is illustrated in Fig. 8.

As shown in Fig. 8, polypropylene with 0.1 luffa fibers revealed a yield strength of 3.01 MPa at 0.139%, followed by a significant stress increment where a 22.6 MPa ultimate tensile strength was exhibited at 2.87%, right before its failure at 2.91%. Figure 9 displays the stress and strain behavior of palm/HDPE NFC at 0.3.

As displayed in Fig. 9, HDPE NFC with 0.3 palm fibers exhibited a yield strength of 1.47 MPa at 0.053%, thereby the stress increased to reach an ultimate tensile strength of 11.1 MPa at 6.09%, followed by a notable decrease throughout the necking phase, hence a ductile failure was exhibited

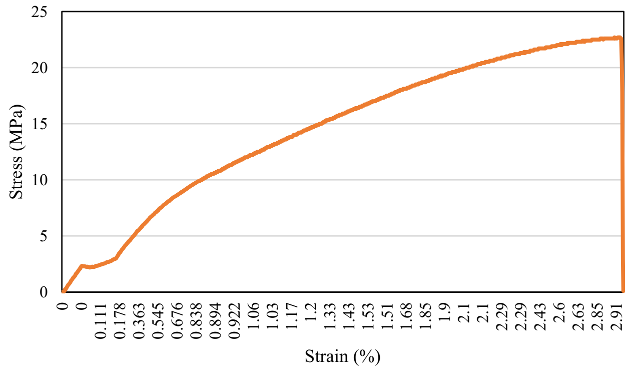

Fig. 8 stress and strain curve of luffa/PP "0.1"

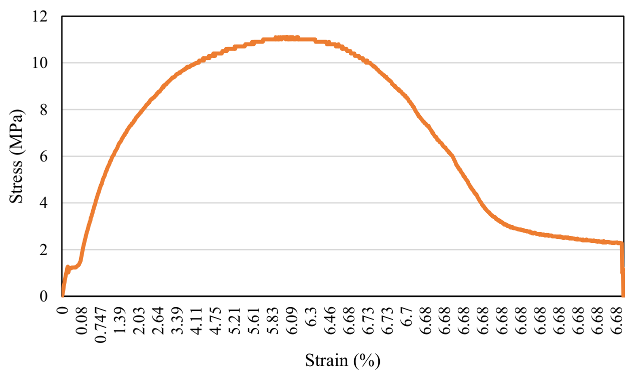

Fig. 9 Stress and strain curve of palm/HDPE "0.3"

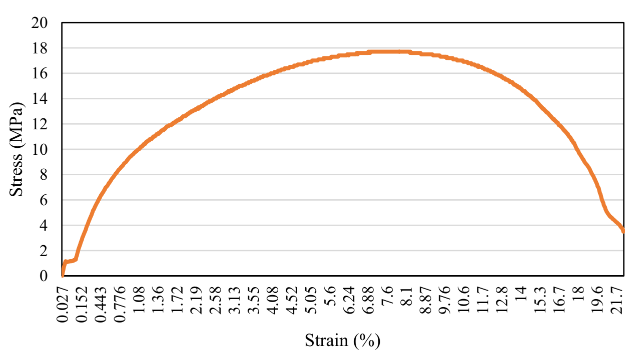

Fig. 10 Stress and strain curve of luffa/HDPE "0.1"

at 6.7%. Figure 10 shows the stress–strain behavior of high-density polyethylene reinforced with 0.1 luffa fibers.

As observed in Fig. 10, a yield strength of 1.28 MPa was observed at 0.027%, then a gradual increase in the stress was observed along with an increase in the strain to reach an ultimate tensile strength of 17.7 at 7.15%. Hence, the stress followed a descending trend till its ductile failure at 21.7%. It is worthy to mention that natural fibers composites with HDPE matrix revealed the highest ductility.

Table 2 Tensile test results

Matrix	Fibers	V_f	TS (MPa)	Strain (%)	E (MPa)
BioPoxy	Palm	0.1	20.800	1.24765	1667.134
		0.2	23.600	1.3597	1399.548
		0.3	21.050	2.3325	1516.204
Epoxy	Palm	0.1	2.370	7.6615	30.934
		0.2	3.323	9.081667	36.594
		0.3	4.343	9.971333	43.558
PP	Palm	0.1	25.233	3.986667	645.408
		0.2	22.467	3.834667	662.295
		0.3	21.100	2.391	686.274
HDPE	Palm	0.1	16.967	11.13833	152.327
		0.2	15.400	9.224	166.956
		0.3	12.567	7.746	162.234
BioPoxy	Luffa	0.1	33.167	3.266667	1015.306
		0.2	35.133	1.281667	1792.263
		0.3	35.300	2.4735	1427.128
Epoxy	Luffa	0.1	2.853	16.36	17.441
		0.2	3.097	16.48	18.790
		0.3	3.687	17.08333	21.580
PP	Luffa	0.1	22.567	2.646333	852.752
		0.2	21.300	3.654	582.923
		0.3	18.333	2.555667	717.360
HDPE	Luffa	0.1	16.600	7.764	213.807
		0.2	15.433	7.600333	203.061
		0.3	10.123	5.11	198.108

As shown in Table 2, natural fibers' reinforced BioPoxy displayed the highest tensile strengths along with the least strain values. While palm as well as luffa reinforced epoxy exhibited the lowest TS compared to the selected matrixes, yet it provided the highest strain record in this study. Moreover, PP matrix revealed a notable TS (between 18 and 25 MPa), while the tensile strength of HDPE samples ranged between 10 and 17 MPa.

As illustrated in Fig. 11, In terms of BioPoxy/palm NFC, the tensile strength increased from 20.8 MPa to 23.6 by increasing the fibers volume fraction from 0.1 to 0.2, thus it decreased back to 21.05 MPa by reaching 0.3. Whereas reinforcing BioPoxy with Luffa fibers exhibited the highest TS outcome in this research, increasing the fibers volume fraction of luffa from 0.1 to 0.3 increased the tensile strength from 33.16 to 35.5 MPa respectively. It worthy to mention that TS of pure BioPoxy 36 is 57.9 MPa. However, highest TS observed in BioPoxy/palm was 23.6 MPa at 0.2, and in BioPoxy/luffa was 35.3 MPa at 0.3. Addition of luffa fibers into BioPoxy resin contributed in higher tensile strengths compared to palm fibers.

As Exhibited in Fig. 12, Epoxy with 0.1 palm exhibited a tensile strength of 2.37 MPa, by growing the fibers' content, TS increased to 3.32 MPa at 0.2 and 4.34 MPa at

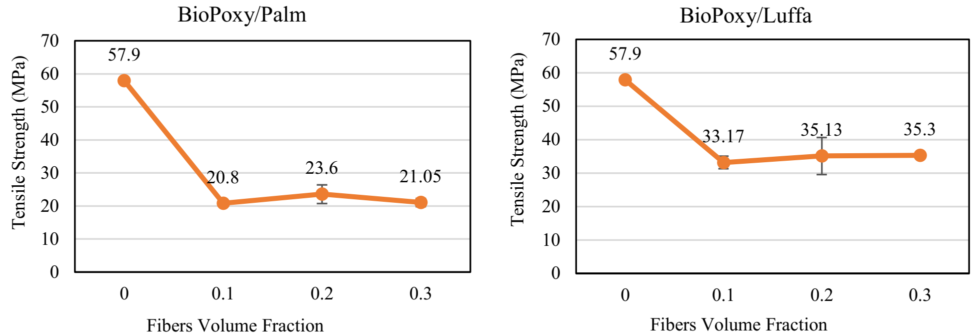

Fig. 11 Tensile strength variation of biopoxy/palm and biopoxy/luffa

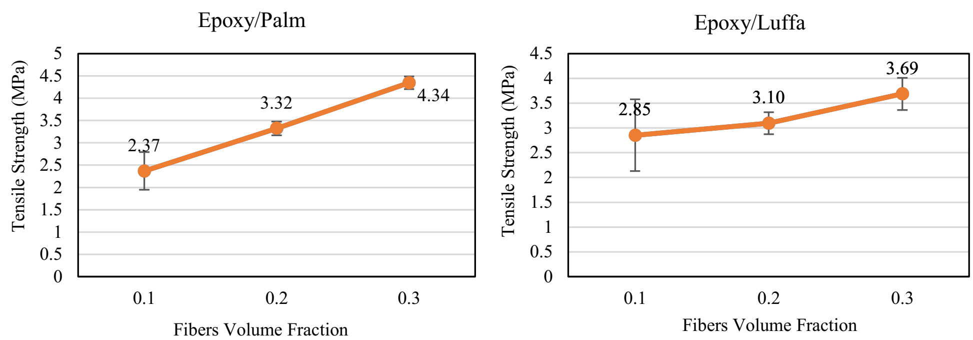

Fig. 12 Tensile strength variation of epoxy/palm and epoxy/luffa

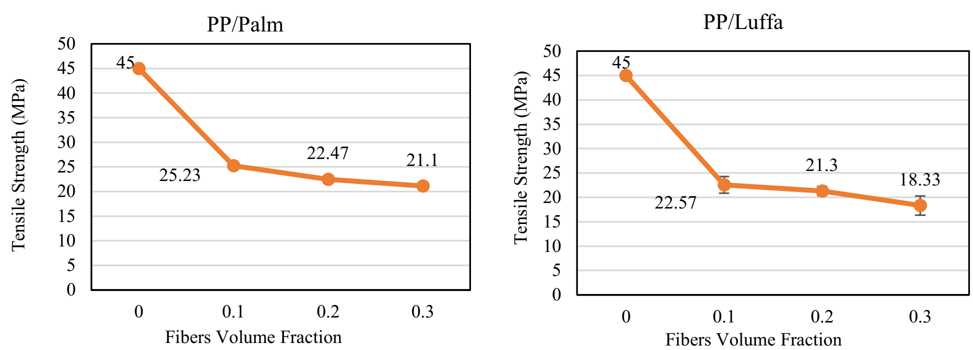

Fig. 13 Tensile strength variation of PP/Palm and PP/luffa

0.3. While luffa reinforced epoxy displayed a TS 2.85 MPa at 0.1 fibers' volume fraction, then reached 3.69 MPa by growing the fibers content up to 0.3. Adding luffa as well as palm fibers into epoxy matrix improves the tensile strength, yet, palm had a better impact than luffa fibers. Highest TS observed in NF reinforced epoxy was 4.34 MPa in epoxy with 0.3 palm fibers.

Regarding palm fibers reinforced polypropylene, as shown in Fig. 13 increasing the fibers' content from 0.1 to 0.3 decreased the tensile strength from 25.23 to 21.1 MPa respectively. Similarly, increasing V_f of luffa fibers in PP reduced TS from 22.57 MPa at 0.1 to 18.33 MPa at 0.3 respectively. Furthermore, addition of palm fibers in PP matrix resulted greater TS values than that of PP/luffa, thus peak TS was 25.23 MPa observed in PP with 0.1 palm fibers. It is worthy to mention that the tensile test findings of PP/luffa were in accordance with Demir et al. [53] at 0.1 fibers' volume fraction, whereas the results of PP/palm agreed with the findings of Otaibi et al. [54] at 10 wt%.

As clearly shown in Fig. 14, loading palm fibers into HDPE matrix reduced the tensile strength to 12.57 MPa at a volume fraction of 0.3, yet it was 16.97 MPa at 0.1 and 15.4 MPa at 0.2. Reinforcing HDPE with luffa fibers reduced the tensile strength from 16.6 MPa at 0.1 to 10.12 MPa at 0.3 respectively. HDPE/palm and HDPE/luffa exhibited identical TS values at 0.1 and 0.2 fibers' volume fraction, whilst palm fibers had a better effect at 0.3. Results of HDPE/palm agreed with mulinari et al. [55] at 10 wt% and Mahdavi et al. [56] at 20 wt%. However, the observed results highlight the potential of palm/biopoxy to be used in industrial applications, luffa/biopoxy for aircraft minor components, palm/epoxy and luffa/epoxy for appliances coating applications, palm/PP and luffa/PP for automotive parts, and palm/HDPE and luffa/HDPE for bio-packaging.

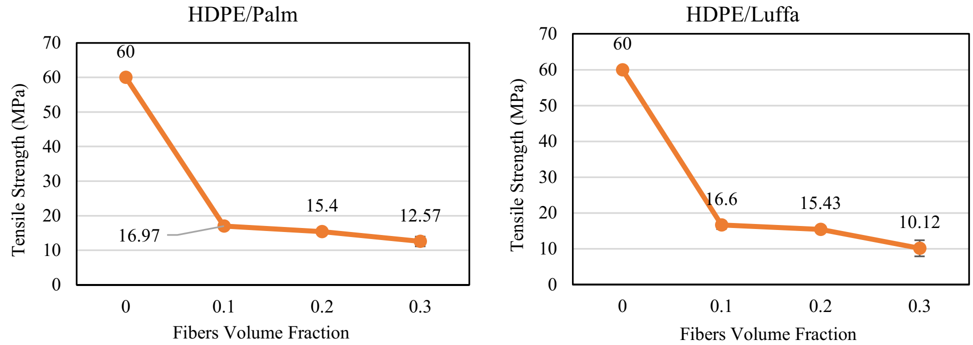

Fig. 14 Tensile strength variation of HDPE/palm and HDPE/luffa

FEA and Experimental Results

Since RVE chopped was observed to be the most accurate model due to its non-linear trends and its agreement with the literature, this model was involved in analyzing the elastic properties of the materials utilized for conducting the tensile test. In ANSYS Explicit Dynamics space, orthotropic output of RVE chopped was assigned as an input into a 120 × 20 × 5 mm beam following ASTM D3039 (Fig. 15). After meshing the sample with linear elements order, the total number of nodes was 693 and the number of elements was 384. Moreover, bottom of the sample was fixed through applying a nodal displacement of 0 mm, and a nodal force was applied on the top of the sample similar to the real tensile test. Furthermore, all models were analyzed by firstly applying a low nodal force on the beam, thereby increasing it till its failure in order to measure its tensile strength. However, each natural fiber composite required different nodal force to break the sample. Figure 15 shows FEA beam model of (a) palm/biopoxy at 0.2, (b) palm/Epoxy at 0.3, (c) palm/PP at 0.1, (d) palm/HDPE at 0.1, (e) luffa/biopoxy at 0.1, (f) luffa/epoxy at 0.3, (g) luffa/PP at 0.2, and (h) luffa/HDPE at 0.1.

This section compares the tensile strength obtained through RVE chopped model followed by FEA simulation, and the conducted experiment. As shown in Fig. 16, experimental tensile strength of BioPoxy/palm increased from 20.8 MPa to 23.6 MPa by increasing the fibers' volume fraction from 0.1 to 0.2, then it dropped to reach a TS of 21.050 MPa at 0.3. A common behavior was displayed by FEA model, TS increased from 20.617 to 22.726 MPa at 0.2, thereby decreased to 22.28 MPa at 0.3. Whereas experimental TS of biopoxy/luffa increased from 33.17 to 35.3 MPa through increasing V_f from 0.1 to 0.3, similarly FEA tensile strength followed an ascending trend to reach a TS value of 33.011 MPa at 0.3. Tensile strength results obtained from FEA showed a good agreement with the experimental findings.

As shown in Fig. 17, both methods showed increasing trends while increasing the fibers' content of luffa as well as palm. However, tensile strength of epoxy/palm observed in FEA model increased from 2.45 to 3.31 MPa by increasing V_f from 0.1 to 0.2, and to 3.79 MPa by increasing V_f up to 0.3, whilst the experimental TS of epoxy/palm increased to 3.32 MPa and 4.34 MPa respectively. In terms of epoxy/luffa, the numerically observed tensile strength increased to 3.17 MPa at 0.2, and 3.47 MPa from 0.2 to 0.3, thus the corresponding experimental results rose to 3.1 MPa by increasing the fibers' volume fraction from 0.1 to 0.2, and 3.69 MPa from 0.2 to 0.3. FEA findings significantly agreed with the tensile test results.

As seen in Fig. 18, considering both FEA and experimental results, increasing the fibers' content to 0.3 decreased TS of both PP/palm and PP/luffa, respectively. Experimental TS of PP/palm NFC, increasing V_f to 0.3 reduced the tensile strength to 22.47 MPa and 21.1 MPa respectively, similarly FEA TS followed a descending trend, TS decreased from 24.274 to 22.3 MPa by increasing the fibers' content to 0.2, and to 15.423 MPa at 0.3. While Regarding TS of PP/luffa, both methods displayed a continuous decline in tensile strength while increasing the fibers volume fraction. Moreover, the simulation results notably agreed with the experimental findings.

As shown in Fig. 19, increasing V_f of palm from 0.1 to 0.2 in HDPE matrix decreased the tensile strength from 16.97 to 15.622 MPa, consequently it decreased to 12.57 MPa at 0.3, similarly TS of HDPE/palm observed in FEA model exhibited a continuous decline to reach a TS value of 11.375 MPa at 0.3. Furthermore, addition of luffa fibers in HDPE reduced the tensile strength, that was observed through FEA simulation as well as FEA model. It is worthy to mention that the overall agreement between FEA simulation and tensile test results is quite acceptable [57, 58]. Although FEA and experimental TS were following same trends in PP/luffa and HDPE/luffa, the predicted values were slightly lower than the experimental.

Machine Learning Findings

Artificial neural network, multiple linear regression, support vector machine, and adaptive neuro-fuzzy inference system were adapted in this research to determine

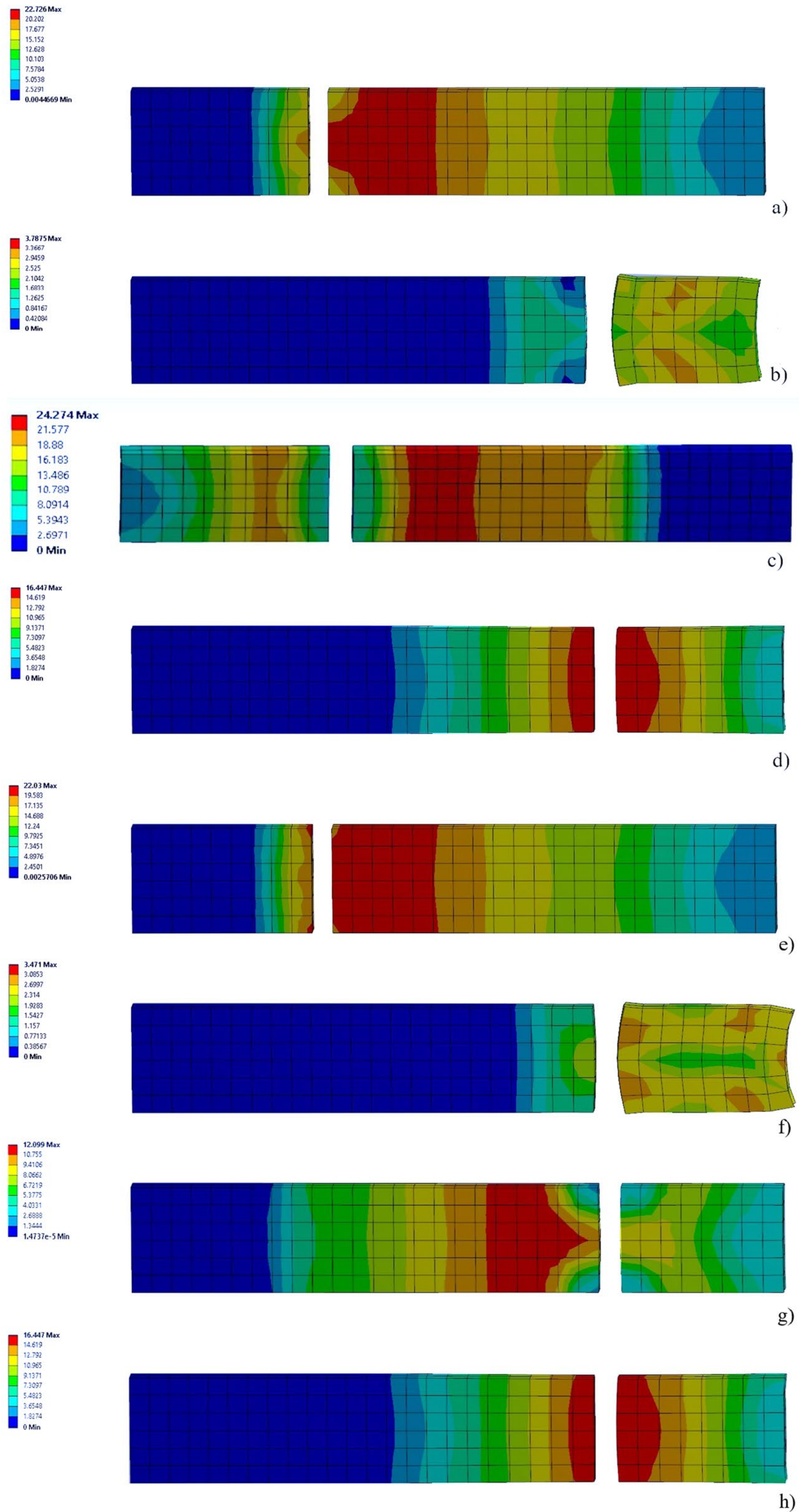

Fig. 15 FEA beam model following ASTM D3039 of **a** 0.2 Palm/biopoxy, **b** 0.3 Palm/epoxy, **c** 0.1 Palm/PP, **d** 0.1 palm/HDPE, **e** 0.1 luffa/biopoxy, **f** 0.3 luffa/Epoxy, **g** 0.2 luffa/PP, and **h** 0.1 luffa/HDPE

the design space as well as to specify most convenient Machine Learning (ML) approach in predicting TS of NFCs. This section introduces the outcome of the aforementioned ML tools in predicting the tensile strength of palm NFCs as well as luffa NFCs. Levenberg–Marquardt algorithm was utilized in this research for training all components of ANN prediction model, which exhibited a swift and stable convergence. The design of the ANN model is

Fig. 16 Experimental versus FEA tensile strength of biopoxy/palm and biopoxy/luffa

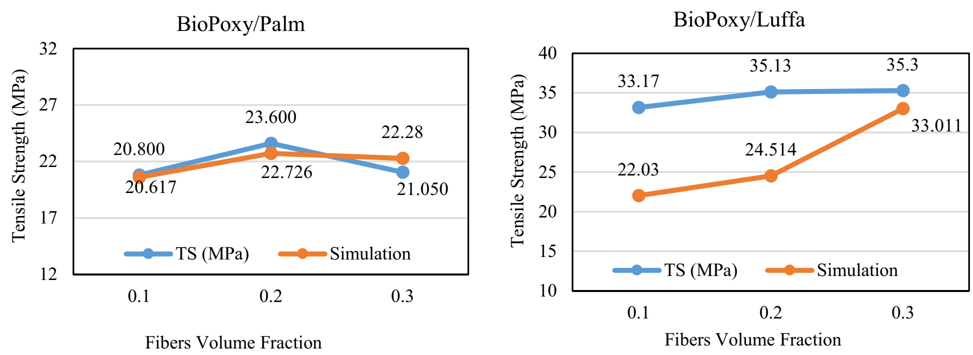

Fig. 17 Experimental versus FEA tensile strength of epoxy/palm and epoxy/luffa

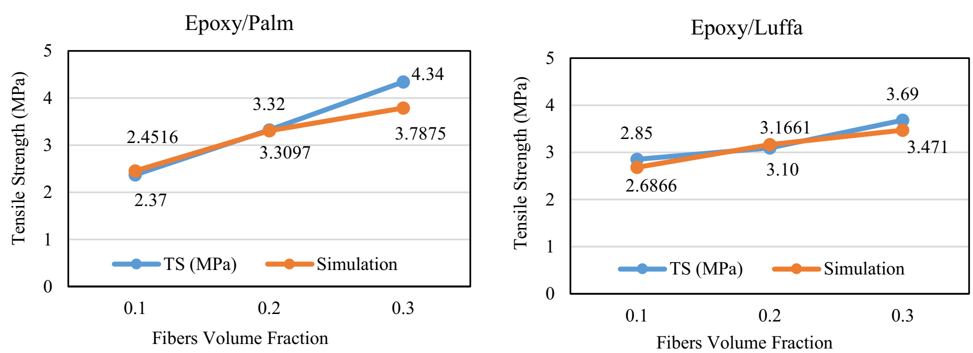

Fig. 18 Experimental versus FEA tensile strength of PP/palm and PP/luffa

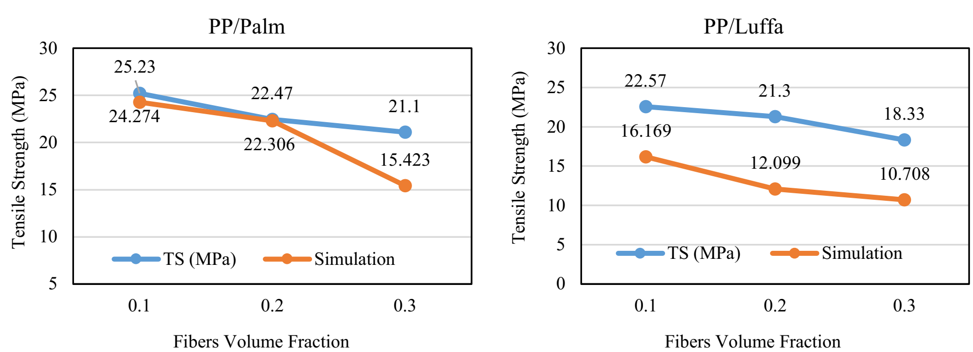

Fig. 19 Experimental versus FEA tensile strength of HDPE/palm and HDPE/luffa

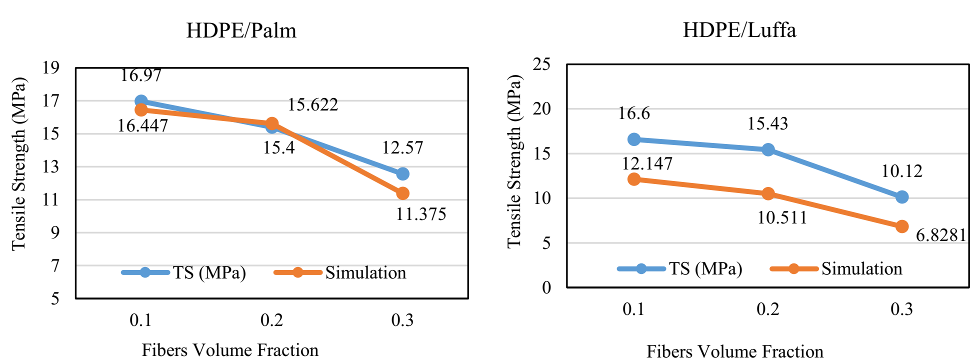

shown in Fig. 20 The model includes 3 inputs, 8 hidden layers, and 1 output.

The model was generated using neural network fitting tool in MATLAB. Input data consisted of: matrix type, fibers' type, and fibers' volume fraction, while the output was tensile strength. Data of all experimentally tested NFC specimens were considered, 70% of the data were used for training the model, 15% for testing, and 15% for validation. Figure 21 displays the schemes of tensile strength regressions for all considered NFCs throughout three different

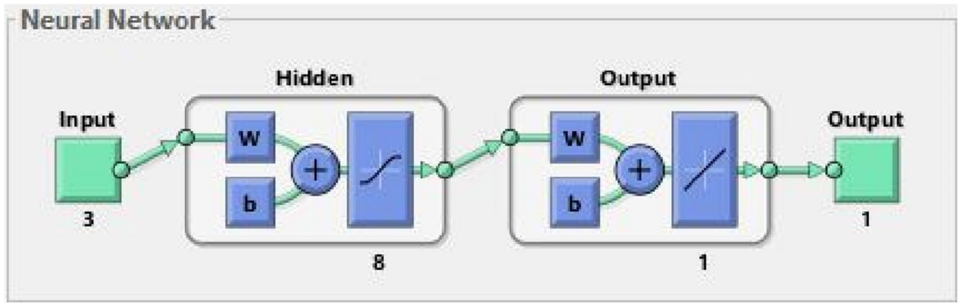

Fig. 20 Artificial neural network model structure

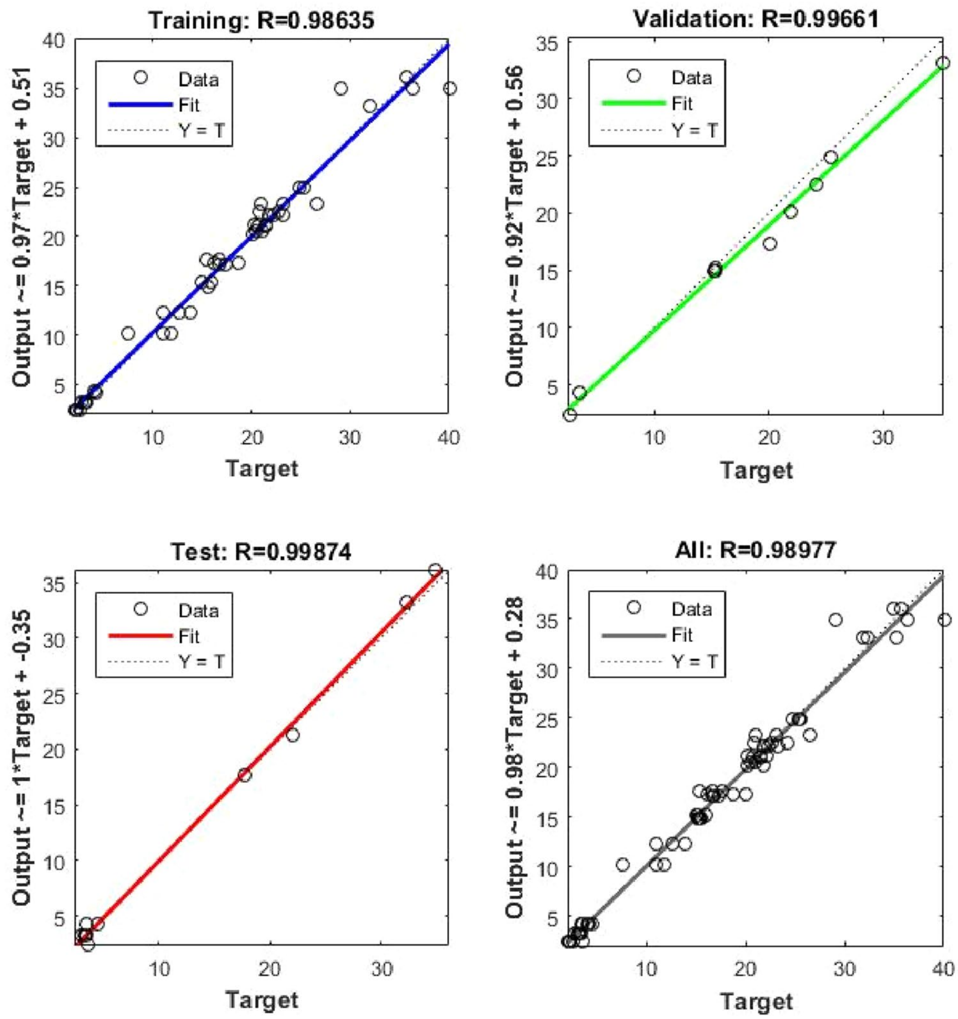

Fig. 21 Regression plot of ANN model

fibers' volume fractions i.e. 0.1, 0.2, and 0.3. This figure highlights the correlation between the ANN output and the experimental data (target).

The correlation between the output values and target values were represented through the solid line, while best correlation that can be generated is represented through the dotted line. The overall regression coefficient of ANN model was observed to be 0.989, which means it is satisfactory as it is close to 1. In this research, regression model was implemented using curve fitting tool in MATLAB. In order to reach a better curve fitting results, two different response surface models were generated using cubic polynomial approximation functions, one for palm NFCs and the other for luffa NFCs. Therefore, input data included matrix type and fibers volume fraction, whereas the output was the corresponding TS values. Moreover, response surface metamodel provides a surface fitting that covers the design in order to predict responses for inputs not considered throughout the

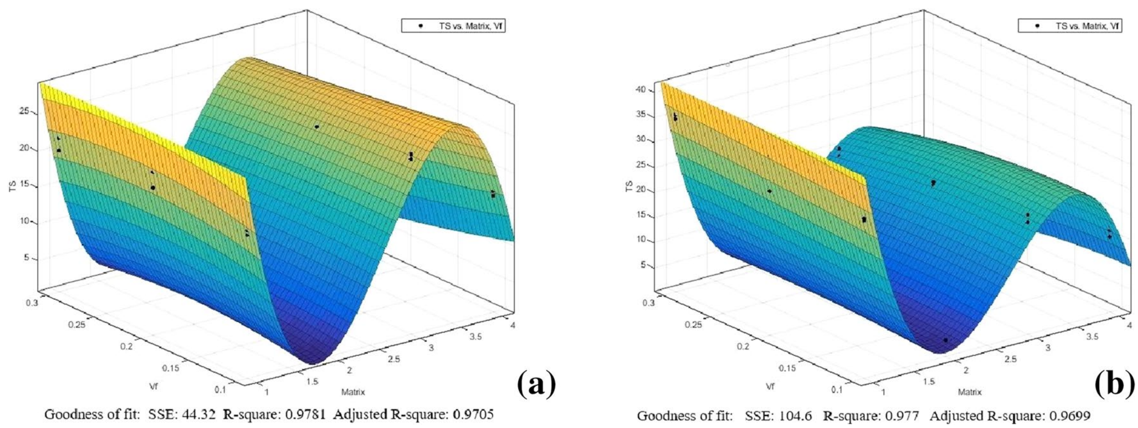

Fig. 22 Response surface fitting of **a** Palm NFCs, and **b** Luffa NFCs

experiment. A cubic polynomial approximation function is involved in study to develop the response surfaces shown in Fig. 22a, b.

MATLAB cftool was utilized for developing the RSM for TS of palm NFCs as well as luffa NFCs. Goodness of fit were evaluated using sum of square error (SSE), R-square adjusted, and root mean square error (RMSE). The values of R-square adjusted ranges between 0 and 1, where a good fit would get a value close 1. In contrast, RMSE and SSE values should be close to zero in order to have a good surface fit. The goodness of fit included an SSE of 44.32, R-square of 0.9781, Adjusted R-square of 0.9705 and RMSE of 1.388. While regarding the RSM model of luffa NFCs, the SSE: 104.6, R-square: 0.977, Adjusted R-square: 0.9699, and RMSE: 2.006. The considered ANFIS model consists of; 3 inputs (matrix type, fibers' type, and V_f), 4 membership function for the first input, 2 for the second input, and 3 membership functions for the third input. Structure of the ANFIS model is illustrated in Fig. 23.

Neuro fuzzy designer tool in MATLAB was utilized for applying ANFIS model. 80% of the experimental results were utilized for training the model and the remaining 20% were used for the testing. All fibers, matrixes, and fibers' volume fractions were considered. FIS model was generated using Gaussmf membership function with a constant output. Training was completed at epoch 2, and average testing error was observed to be 1.4876. ANFIS model plot that displays the training data as well as the FIS output data is shown in Fig. 24.

The support vector machine model in this research was generated through regression learner tool in MATLAB. 4 Matrix types, 2 fibers' type, and 3 fibers volume fraction were considered as input parameters. Figure 25 shows the training and testing output datasets developed by the SVM model. Blue dotes illustrates the true data, while the yellow dots are the predicted data.

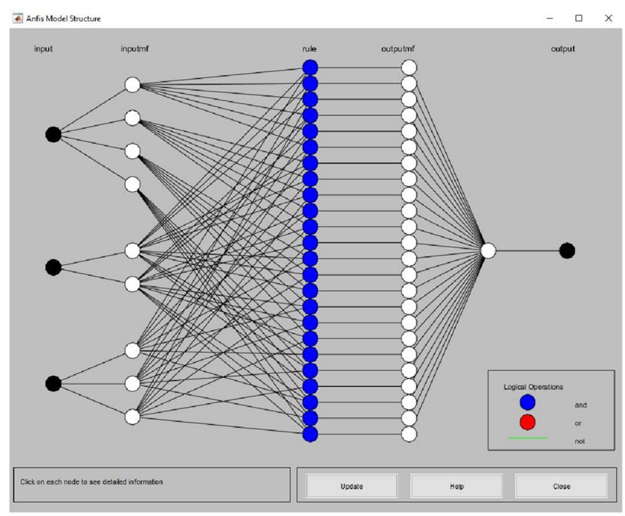

Fig. 23 ANFIS model structure

Hence, experimental results of all NFCs were utilized for training the SVM model, the kernel function used was the Gaussian, and the involved preset was the fine Gaussian SVM. Moreover, the obtained RMSE was 2.7296, R-squared was 0.93, and MSE was 7.4509. Table 3 shows the predicted data using machine learning methods as well as real tensile strength results of palm and luffa NFCs.

As clearly shown in Table 3 the predicted TS using ANN, and ANFIS, displayed a strong agreement with experimental results with a prediction error of 3.21% and 2.17%, respectively, whilst TS values obtained through MLR and SVM showed a decent agreement with an error of 6.86% and 12.65%. That emphasizes that these models are able to be trained and involved in assuming the tensile strength of natural fibers composite materials. Furthermore, luffa/BioPoxy at 0.3 V_f revealed the highest tensile strength values throughout all the considered ML approaches. Most suitable

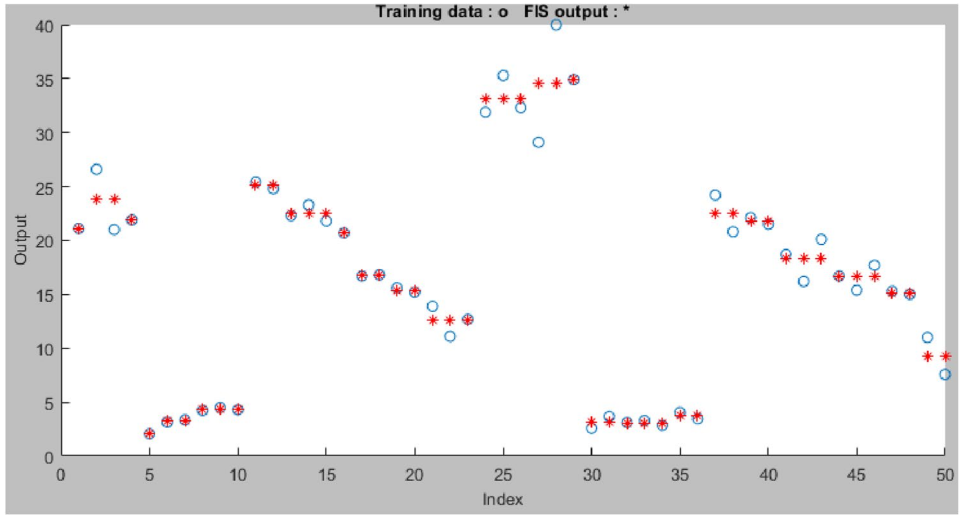

Fig. 24 Adaptive Neuro-Fuzzy inference system plot

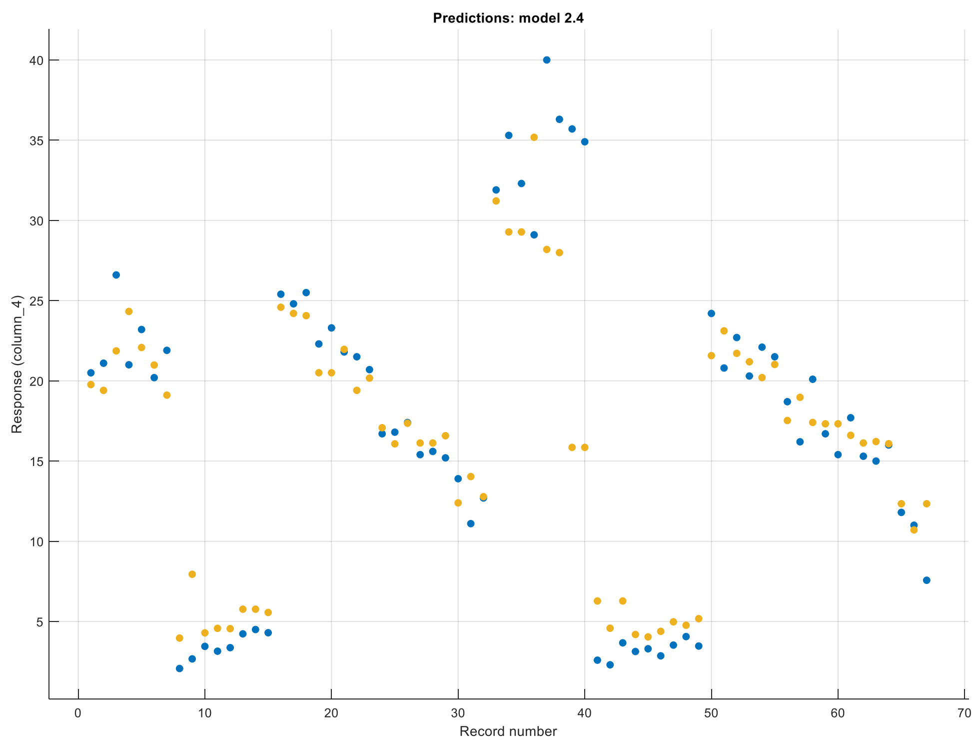

Fig. 25 Predict versus real SVM data

machine learning approach for predicting tensile strength of natural fibers composites is ANFIS as it showed least prediction error "2.17%".

Conclusion

This research presents an investigation on the mechanical properties of luffa and palm NFCs in Epoxy, Ecopoxy "BioPoxy 36", PP and HDPE matrixes. RVE chopped model was considered for analyzing the orthotropic properties of palm and luffa NFCs, thereby, the output of RVE chopped was assigned into a 120 × 20 × 5 mm beam as for ASTM D3039, and loaded under tensile load till failure. Moreover, experimental tensile test was conducted for testing the tensile properties of the considered NFCs as well as validating the simulation results. Thus, different machine learning techniques were implemented in order to identify the design space i.e. Artificial neural network, multiple linear regression, adaptive neuro-fuzzy inference system, and support vector machine. Effect of increasing fiber content in the matrix was taken into account by considering several fibers' volume fractions, from 0.1 to 0.5 in model validation and from 0.1 to 0.3 V_f for the simulation, experiment

Table 3 Predicted tensile strength using ANN, MLR, ANFIS, and SVM

Matrix	Fibers	V_f	Experimental TS (MPa)	ANN TS (MPa)	MLR TS (MPa)	ANFIS TS (MPa)	SVM TS (MPa)
BioPoxy 36	Palm	0.1	20.800	20.550	20.810	21.100	19.835
BioPoxy 36	Palm	0.2	23.600	23.250	22.851	23.800	22.256
BioPoxy 36	Palm	0.3	21.050	20.150	21.943	21.900	20.646
Epoxy	Palm	0.1	2.370	2.423	3.090	2.070	3.928
Epoxy	Palm	0.2	3.323	3.275	3.906	3.260	4.411
Epoxy	Palm	0.3	4.343	4.235	3.027	4.343	5.489
PP	Palm	0.1	25.233	24.850	23.887	25.100	24.242
PP	Palm	0.2	22.467	22.150	23.055	22.467	22.043
PP	Palm	0.3	21.100	20.950	21.783	20.700	20.245
HDPE	Palm	0.1	16.967	17.110	17.502	16.750	16.828
HDPE	Palm	0.2	15.400	14.900	14.600	15.400	16.459
HDPE	Palm	0.3	12.567	12.320	12.513	12.567	12.642
BioPoxy 36	Luffa	0.1	33.167	33.150	33.188	33.167	31.041
BioPoxy 36	Luffa	0.2	35.133	34.980	34.674	34.550	30.356
BioPoxy 36	Luffa	0.3	35.300	36.090	35.828	34.900	33.637
Epoxy	Luffa	0.1	2.853	2.419	3.040	3.130	3.852
Epoxy	Luffa	0.2	3.097	3.282	3.624	3.097	4.370
Epoxy	Luffa	0.3	3.687	4.266	2.912	3.765	4.730
PP	Luffa	0.1	22.567	22.440	22.042	22.500	22.060
PP	Luffa	0.2	21.300	21.210	21.535	21.800	20.835
PP	Luffa	0.3	18.333	17.370	18.768	18.333	17.460
HDPE	Luffa	0.1	16.600	17.630	17.116	16.600	16.661
HDPE	Luffa	0.2	15.433	15.280	15.328	15.150	16.255
HDPE	Luffa	0.3	10.123	10.230	10.318	9.285	10.546
Prediction error %				3.21%	6.86%	2.17%	12.65%

and machine learning models. Regarding the experimental tensile test, NFCs with biopoxy matrix showed the greatest tensile strength values and lowest strain, whereas NFCs with epoxy matrix displayed least tensile strengths in this research with highest strain values.

Furthermore, NFCs with PP matrix exhibited significant tensile strength values ranging between 18 and 25 MPa. TS of NFCs with HDPE matrix ranged from 10 to 17 MPa. Peak tensile strength observed in luffa/BioPoxy at 0.3 with a value of 35.5 MPa. Increasing the fibers' volume fraction from 0.1 to 0.2 of natural fibers' reinforced biopoxy increased TS then decreased at 0.3. Reinforcing BioPoxy with luffa fibers showed better properties compared to date palm fibers. Growing the content of palm as well as luffa fibers' up to 0.3 increased the tensile strength of epoxy. Peak TS in natural fibers' reinforced epoxy was 4.34 MPa in palm/epoxy at 0.3. While addition of luffa and palm fibers decreases the tensile strength of HDPE and PP matrixes, however, palm revealed higher TS values in PP (25.23 MPa at 0.1) and in HDPE (16.97 MPa at 0.1). Based on the revealed results, palm/BioPoxy can be utilized for industrial applications, luffa/BioPoxy can be used for producing aircraft components, luffa/epoxy and palm/epoxy can be involved in appliances' coating, while luffa/PP and palm/PP have the ability to emerge in automotive parts' production. It is worthy to mention that simulation results significantly agreed with the tensile test findings, where these FEA results followed the exact same trends observed in the experimental findings, as well as majority of the TS values were in accordance. Furthermore, in terms of machine learning application, predicted tensile strengths through ANN, and ANFIS drastically agreed with the experimental outcome, having a prediction error of 3.21% and 2.17%. Whereas tensile strength predicted using MLR and SVM displayed an acceptable agreement with a prediction error of 6.86% and 12.65%. Which therefore provides evidences the capability of these machine learning models of being trained and utilized for predicting TS of natural fibers composites. Moreover, throughout all the considered ML approaches, highest tensile strength values were revealed in luffa/BioPoxy at 0.3 V_f. ANFIS can be considered as suitable machine learning approach for predicting tensile strength of natural fibers composites as it exhibited lowest prediction error.

Funding The authors have not disclosed any funding.

Declarations

Conflict of interest The authors declare that they have no conflict of interest.

References

1. Jauhari N, Mishra R, Thakur H (2015) Mater Today 2:2868–2877. https://doi.org/10.1016/j.matpr.2015.07.304
2. Zhan J, Li J, Wang G, Guan Y, Zhao G, Lin J, Naceur H, Coutellier D (2021) Polym Compos 42:1305–1324. https://doi.org/10.1002/pc.25902
3. Wang H, Yang L, Wu H (2021) Polym Compos 42:714–723. https://doi.org/10.1002/pc.25860
4. Ku H, Wang H, Pattarachaiyakoop N, Trada M (2011) Compos B Eng 42:856–873. https://doi.org/10.1016/j.compositesb.2011.01.010
5. Sanjay MR, Madhu P, Jawaid M, Senthamaraikannan P, Senthil S, Pradeep S (2018) J Clean Prod 172:566–581. https://doi.org/10.1016/j.jclepro.2017.10.101
6. Fan F, Safaei B, Sahmani S (2021) Thin-Walled Struct 159:107231. https://doi.org/10.1016/j.tws.2020.107231
7. Fan F, Sahmani S, Safaei B (2021) Compos Struct 255:112969. https://doi.org/10.1016/j.compstruct.2020.112969
8. Safri SNA, Sultan MTH, Jawaid M, Jayakrishna K (2018) Compos B Eng 133:112–121. https://doi.org/10.1016/j.compositesb.2017.09.008
9. Nguong C, Lee S, Sujan D (2013) WASET 7:52–59. https://doi.org/10.5281/zenodo.1332600
10. Yan L, Chouw N, Jayaraman K (2014) Compos B Eng 56:296–317. https://doi.org/10.1016/j.compositesb.2013.08.014
11. Sathishkumar TP, Navaneethakrishnan P, Shankar S, Rajasekar R, Rajini N (2013) J Reinf Plast Compos 32:1457–1476. https://doi.org/10.1177/0731684413495322
12. Safaei B (2020) Steel Compos Struct 35:659–670. https://doi.org/10.12989/scs.2020.35.5.659
13. Kong C, Lee H, Park H (2016) Compos B Eng 91:18–26. https://doi.org/10.1016/j.compositesb.2015.12.033
14. Koronis G, Silva A, Fontul M (2013) Compos B Eng 44:120–127. https://doi.org/10.1016/j.compositesb.2012.07.004
15. Elanchezhian C, Ramnath BV, Ramakrishnan G, Rajendrakumar M, Naveenkumar V, Saravanakumar MK (2018) Mater Today 5:1785–1790. https://doi.org/10.1016/j.matpr.2017.11.276
16. Kiruthika AV (2017) J Build Eng 9:91–99. https://doi.org/10.1016/j.jobe.2016.12.003
17. Mazzanti V, Pariante R, Bonanno A, Ruiz de Ballesteros O, Mollica F, Filippone G (2019) Compos Sci Technol 180:51–5910. https://doi.org/10.1016/j.compscitech.2019.05.015
18. Wang Y, Ermilov V, Strigin S, Safaei B (2021) Microsyst Technol 27:4241–4251. https://doi.org/10.1007/s00542-021-05218-z
19. Fattahi A, Safaei B, Qin Z, Chu F (2021) Steel Compos Struct Int J 38:177–187. https://doi.org/10.12989/scs.2021.38.2.177
20. Alhijazi M, Safaei B, Zeeshan Q, Asmael M, Eyvazian A, Qin Z (2020) Sustainability 12:7683. https://doi.org/10.3390/su12187683
21. Pires C, Motta LAdC, Ferreira RAdR, Caixeta CdO, Savastano H (2020) J Nat Fibers 17:1–13. https://doi.org/10.1080/15440478.2020.1726245
22. Shalwan A, Yousif B (2014) Mater Des 59:264–273. https://doi.org/10.1016/j.matdes.2014.02.066
23. Ibrahim H, Farag M, Megahed H, Mehanny S (2014) Carbohydr Polym 101:11–19. https://doi.org/10.1016/j.carbpol.2013.08.051
24. Shen J, Xie YM, Huang X, Zhou S, Ruan D (2013) Int J Impact Eng 57:17–26. https://doi.org/10.1016/j.ijimpeng.2013.01.004
25. Mani P, Dellibabu G, Anilbasha K, Anbukarsi K (2014) Int J Eng Res Technol 3(1882):1885. https://doi.org/10.17577/IJERTV3IS051784
26. Alhijazi M, Zeeshan Q, Qin Z, Safaei B, Asmael M (2020) Nanotechnol Rev 9:853–875. https://doi.org/10.1515/ntrev-2020-0069
27. Behzad T, Sain M (2007) Compos Sci Technol 67:1666–1673. https://doi.org/10.1016/j.compscitech.2006.06.021
28. Azizi S, Safaei B, Fattahi AM, Tekere M (2015). Adv Mater Sci Eng. https://doi.org/10.1155/2015/318539
29. Prasad V, Joy A, Venkatachalam G, Narayanan S, Rajakumar S (2014) Procedia Eng 97:1116–1125. https://doi.org/10.1016/j.proeng.2014.12.390
30. Sowmya C, Ramesh V, Karibasavaraja D (2018) Mater Today 5:13309–13320. https://doi.org/10.1016/j.matpr.2018.02.323
31. Hemmat Esfe M, Esfandeh S, Bahiraei M (2020) Eng Comput 38:2451–2468. https://doi.org/10.1007/s00366-020-01204-7
32. Alhijazi M, Zeeshan Q, Safaei B, Asmael M, Qin Z (2020) J Polym Environ 28:3029–3054. https://doi.org/10.1007/s10924-020-01842-4
33. Alhijazi M, Safaei B, Zeeshan Q, Asmael M (2021) Polym Compos 42:3508–3517. https://doi.org/10.1002/pc.26075
34. Safaei B, Chukwueloka Onyibo E, Hurdoganoglu D (2022). Facta Universitatis, Series: Mechanical Engineering. https://doi.org/10.22190/FUME220201009S
35. Onyibo EC, Safaei B (2022) Report Mech Eng 3:283–300. https://doi.org/10.31181/rme20023032022o
36. Ghanati P, Safaei B (2019) Indian J Phys 93:47–52. https://doi.org/10.1007/s12648-018-1254-9
37. Pattnaik P, Sharma A, Choudhary M, Singh V, Agarwal P, Kukshal V (2020) Mater Today 44:4703–4708. https://doi.org/10.1016/j.matpr.2020.11.026
38. Safaei B, Chukwueloka Onyibo E, Hurdoganoglu D (2022) Facta Universitatis, Series: Mechanical Engineering. https://doi.org/10.22190/FUME220404027S
39. Safaei B (2021) Eur Phys J Plus 136:646. https://doi.org/10.1140/epjp/s13360-021-01632-4
40. Alibar MY, Safaei B, Asmael M, Zeeshan Q (2021). Arch Comput Method Eng. https://doi.org/10.1007/s11831-021-09669-5
41. Antil SK, Antil P, Singh S, Kumar A, Pruncu CI (2020) Materials 13:1381. https://doi.org/10.3390/ma13061381
42. Pati PR (2019) IJPT 23:253–260. https://doi.org/10.1007/s12588-019-09257
43. Baseer AA, Ravi Shankar D, Hussain MM (2020) Surf Rev Lett 27:1950099. https://doi.org/10.1142/S0218625X19500999
44. Atuanya CU, Nwobi-Okoye CC, Onukwuli OD (2014) Int J Mech Mater Eng 9:1–20. https://doi.org/10.1186/s40712-014-0007-6
45. Daghigh V, Lacy TE Jr, Daghigh H, Gu G, Baghaei KT, Horstemeyer MF, Pittman CU Jr (2020) Mater Today Commun 22:100789. https://doi.org/10.1016/j.mtcomm.2019.100789
46. Daghigh V, Lacy TE Jr, Daghigh H, Gu G, Baghaei KT, Horstemeyer MF, Pittman CU Jr (2020) J Reinf Plast Compos 39:587–598. https://doi.org/10.1177/0731684420915984
47. Garg A, Bordoloi S, Mondal S, Ni J-J, Sreedeep S (2020) J Nat Fibers 17:650–664. https://doi.org/10.1080/15440478.2018.1521763
48. Wang Z, Chegdani F, Yalamarti N, Takabi B, Tai B, El Mansori M, Bukkapatnam S (2020). J Manuf Sci Eng. https://doi.org/10.1115/1.4045945
49. Madhu P, Sanjay M, Senthamaraikannan P, Pradeep S, Saravanakumar S, Yogesha B (2018) J Nat Fibers 16:1132–1144. https://doi.org/10.1080/15440478.2018.1453433

50. Hanan F, Jawaid M, Paridah MT, Naveen J (2020) Polymers 12:2052. https://doi.org/10.3390/polym12092052
51. Bouktif S, Fiaz A, Ouni A, Serhani MA (2018) Energies 11:1636. https://doi.org/10.3390/en11071636
52. Wuest T, Weimer D, Irgens C, Thoben K-D (2016) Prod Manuf Res. 4:23–45. https://doi.org/10.1080/21693277.2016.1192517
53. Demir H, Atikler U, Balköse D, Tıhmınlıoğlu F (2006) Compos Part A Appl Sci Manuf 37:447–456. https://doi.org/10.1016/j.compositesa.2005.05.036
54. Alothman OY, Alrashed MM, Anis A, Naveen J, Jawaid M (2020) Polymers 12:597. https://doi.org/10.3390/polym12030597
55. Mulinari DR, Marina AJ, Lopes GS (2015) IJCME 9:903–906. https://doi.org/10.5281/zenodo.1109177
56. Mahdavi S, Kermanian H, Varshoei A (2010) BioResources 5:2391–2403
57. Chokshi S, Gohil P, Patel D (2020) Mater Today 28:498–503. https://doi.org/10.1016/j.matpr.2019.12.208
58. Balasubramanian K, Rajeswari N, Vaidheeswaran K (2020) Mater Today 28:1149–1153. https://doi.org/10.1016/j.matpr.2020.01.098